

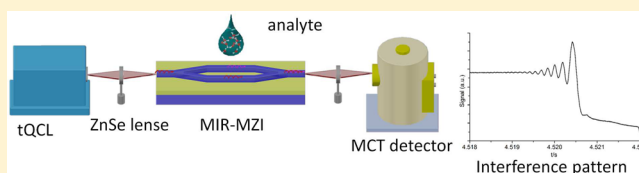
On-Chip Integrated Mid-Infrared GaAs/AlGaAs Mach–Zehnder Interferometer

Markus Sieger,[†] Franz Balluff,[†] Xiaofeng Wang,[†] Seong-Soo Kim,[†] Lothar Leidner,[‡] Guenter Gauglitz,[‡] and Boris Mizaikoff^{*,†}

[†]Institute of Analytical and Bioanalytical Chemistry, University of Ulm, Albert-Einstein-Allee 11, 89075 Ulm, Germany

[‡]Institute of Theoretical and Physical Chemistry, University of Tuebingen, Auf der Morgenstelle 15, 72076 Tuebingen, Germany

ABSTRACT: We report the design, fabrication, and first functional verification of mid-infrared (MIR; 3–12 μm) Mach–Zehnder interferometers (MZIs). The developed MIR-MZIs are entirely chip-integrated solid-state devices based on GaAs/AlGaAs technology waveguide fabricated via conventional optical lithography and reactive ion etching (RIE). Thus, fabricated MIR-MZIs were combined with a broadly tunable quantum cascade laser (tQCL) providing a wavelength coverage of 5.78–6.35 μm . MIR-MZIs have been designed with a waveguide width of 5 μm to ensure single mode behavior, avoiding optically undefined interference patterns. Several structures with different opening angles of the Y-junction were fabricated and tested for maximizing IR radiation throughput. This study demonstrates the feasibility of the very first chip-integrated mid-infrared Mach–Zehnder structures via interference patterns produced by minute amounts of water deposited at different positions of the MIR-MZI structure.



The mid-infrared (MIR; 3–12 μm) spectral range is particularly interesting for biosensing applications, since it provides inherent molecular selectivity. MIR photons interact with most organic and inorganic molecules by excitation of vibrational and rotational modes.¹ Quantum cascade lasers (QCLs) are the most promising light source technology for IR sensing applications due to their compact dimensions, long lifetime, and broad tunability when coupled with an external cavity. Tunable QCLs (tQCLs) are nowadays commercially available across almost the entire MIR band and are in part tunable for a range exceeding 150 cm^{-1} .^{2,3} Consequently, the combination of tQCLs with frequency-matched thin-film MIR waveguides for the first time facilitates the development of miniaturized and potentially fully integrated MIR photonic sensing structures applicable across the entire MIR spectrum within a single on-chip device.

Most photonic devices relevant to analytical applications (i.e., chem-/biosensing) take advantage of the evanescent field generated at the interface between a high-refractive-index waveguide and a low-refractive-index sample medium, which allows direct monitoring of small changes in optical properties such as, e.g., refractive index changes without labeling of the involved species. Among the evanescent field sensors, interferometric arrangements such as, e.g., Mach–Zehnder interferometers (MZIs) are the most suitable devices capitalizing on integrated optics due to their high sensitivity and high level of integration and miniaturization and due to the fact that no moving components are needed. Chemicals or chemical reactions may change the propagation properties of light in optical transducers and within the evanescent field by affecting the absorption coefficient or the refractive index in the vicinity of a light path.^{4,5} Within an integrated MZI structure, photons

propagate along a waveguide and are divided by a symmetric Y-junction into two light beams of equal intensity and phase. After propagating through the parallel-arranged reference and sensor arms, the recombined light waves create an interference pattern (Figure 1). If an analyte or a chemical reaction is

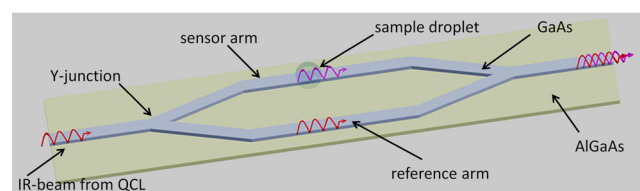


Figure 1. Configuration of a mid-infrared Mach–Zehnder interferometer.

performed at the surface of only one arm, the photons propagating along that arm experience a change in phase. Recombining this signal with the initial wave propagating in the reference arm results in an interference pattern that is dependent on the difference in effective refractive index at both arms. The intensity (I) of the sinusoidal interference signal depends on the interaction length (L) and the difference of the effective refractive indices (ΔN) at the two arms following^{4,5}

$$I \sim [1 + V \cdot \cos \Delta\Phi]$$

Received: September 4, 2012

Accepted: November 6, 2012

Published: November 6, 2012

$\Delta\Phi$ corresponds to the phase shift between the guided modes of the two arms and correlates directly to L and ΔN ; V represents the visibility factor.

$$\Delta\Phi = \frac{2\pi}{\lambda} \cdot L \cdot \Delta N$$

For facilitating data evaluation, the optical device should exhibit monomode behavior. If several modes are present, both variation of the outer medium and interference between the modes create a rather unspecific interference pattern. In comparison to indirect methods based on markers such as, e.g., fluorescence- or radio-labeling, direct absorption-based evanescent field sensing methods usually do not require specific sample preparation, thereby providing substantial potential for direct and real-time detection of interactions or binding of, e.g., biomolecules.⁴ The first biosensing approaches using integrated MZIs were performed using glass substrates by immobilizing a protein adlayer of a three-step biotin–avidin system and analyzing the immobilization of biotinylated immunoglobulins.⁶ Later, Prieto et al.⁵ presented a MZI operating at a wavelength of 633 nm which was fabricated from Si_3N_4 with an excellent sensitivity $(d\Delta\Phi(2\pi)/dn) = 1450$ and implied a detection limit of $\Delta n = 7 \times 10^{-6}$. Due to complementary metal-oxide-semiconductor (CMOS) technology, the device was readily integrated with a microfluidic system facilitating an effective refractive index detection limit of $\Delta n = 2 \times 10^{-7}$, which represents one of the most sensitive measurements obtained by integrated optical interferometric approaches.⁷

Mizaikoff and collaborators have recently reported a new generation of semiconductor GaAs/ $\text{Al}_{0.2}\text{Ga}_{0.8}\text{As}$ IR waveguides with a useful spectral window up to 13 μm .⁸ These thin-film IR waveguides are grown either by molecular beam epitaxy (MBE) or via metal–organic vapor phase epitaxy (MOVPE).⁹ Due to their wide spectral window, these semiconductor waveguides are competitive to currently applied IR-transparent materials such as, e.g., polycrystalline silver halides and amorphous chalcogenide glasses.¹⁰ In the present study, integrated MIR-MZIs have been developed on the basis of GaAs/AlGaAs thin-film waveguide structures. A variety of MZI structures were fabricated and tested in order to optimize the relevant design parameters. Finally, functionality of such MIR-MZIs has been demonstrated, thereby corroborating the potential for a novel chem-/biosensing platform in the field of mid-infrared integrated optics, which is not well established to date.

EXPERIMENTAL SECTION

MIR-MZI devices were microstructured from waveguide layers deposited at the surface of a 1 mm thick GaAs ($n = 3.3$) wafer with a 6 μm thick optical buffer layer comprising $\text{Al}_{0.2}\text{Ga}_{0.8}\text{As}$ ($n = 3.2$) and the actual GaAs waveguiding layer, again with a thickness of 6 μm . The MZI structures were defined via optical photolithography and were fabricated using reactive ion etching (RIE). After spincoating a photoresist (AZ ECI 3027, AZ Electronic Materials, Wiesbaden, Germany) onto the surface, the wafer was exposed to UV radiation via a manual mask aligner. The subsequent development process lead to photoresist MZI patterns, which were then transferred to the wafer via RIE. Afterward, the photoresist pattern was removed, and the back-side of the wafer was polished facilitating individual device cleavage. MZI chips were cleaved along the crystal axis with a diamond knife to obtain chip dimensions of approximately 5 mm in width and 8 mm in length. The waveguide width of the MZIs was selected at 5 μm , thereby

ensuring monomode behavior, which was confirmed by simulations based on the finite element method. To avoid optical coupling between the propagating modes within each MZI arm, the distance between the arms of a MZI was selected at 200 μm . Several structures with different opening angles of the Y-junction ($1\text{--}10^\circ$) were fabricated, thereby optimizing the radiation throughput of the MIR-MZI structure (Figure 2a).

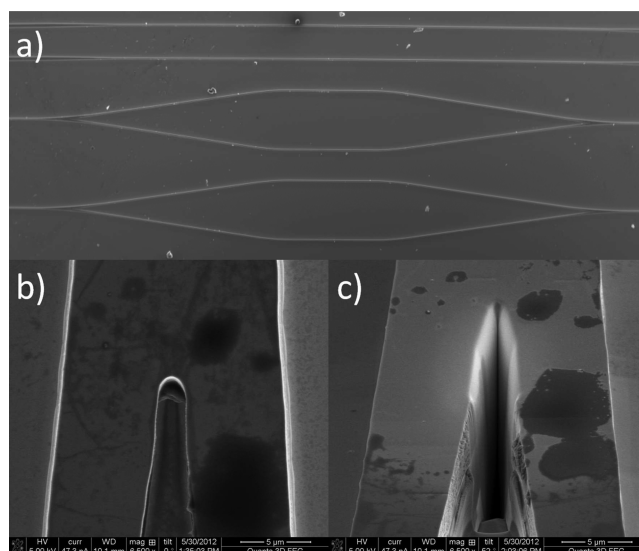


Figure 2. Scanning electron microscopy (SEM) images of MIR-MZI waveguides: (a) top view of GaAs/AlGaAs MZIs with an opening angle of 9° . Y-junction before (b) and (c) after FIB milling process.

Thereafter, the structures were fine-tuned via focused ion beam (FIB) milling for minimizing scattering losses at the Y-junction and to increase the optical throughput (Figure 2b). For avoiding redeposition of Ga, XeF_2 was used as etch enhancing gas during the FIB milling process (Figure 2c).

The optical setup comprised a tunable QCL light source (Daylight Solutions Inc., San Diego, CA, USA) providing MIR radiations in the range of 5.78–6.35 μm . The laser radiation was focused via a ZnSe lens onto the MIR-MZI waveguide entrance facet. A second lens was used to focus radiation emanating at the distal end of the waveguide onto a liquid nitrogen cooled mercury–cadmium–telluride (MCT) detector (Kolmar Technologies, Newbury, MA, USA), which was connected to an oscilloscope and high-speed digital transient recorder (Saturn, AMO GmbH, Aachen, Germany).

First, experimental studies were focused on characterizing the optical throughput of MIR-MZI structures in comparison to straight waveguides (i.e., without Y-junction) fabricated at the same chip. If the opening angle exceeds 6° , almost no radiation was propagated through the device. To date, MIR-MZIs with an angle of the Y-junction at 1° provide maximum throughput, which was further enhanced by polishing the Y-junction via FIB milling.

In order to demonstrate that the developed MIR-MZI structures are indeed functional, sample droplets were deposited at various locations along the MIR-MZI structure (Figure 3a). Small amounts of Millipore water (5 μL droplets) were deposited at the MIR-MZI surface and were analyzed at a wavelength of 1694 cm^{-1} adjusted via the tQCL.

If the droplet was deposited at the incoupling straight waveguide of the MZI structure, no interference pattern was determined. Only an overall decrease in energy throughput due

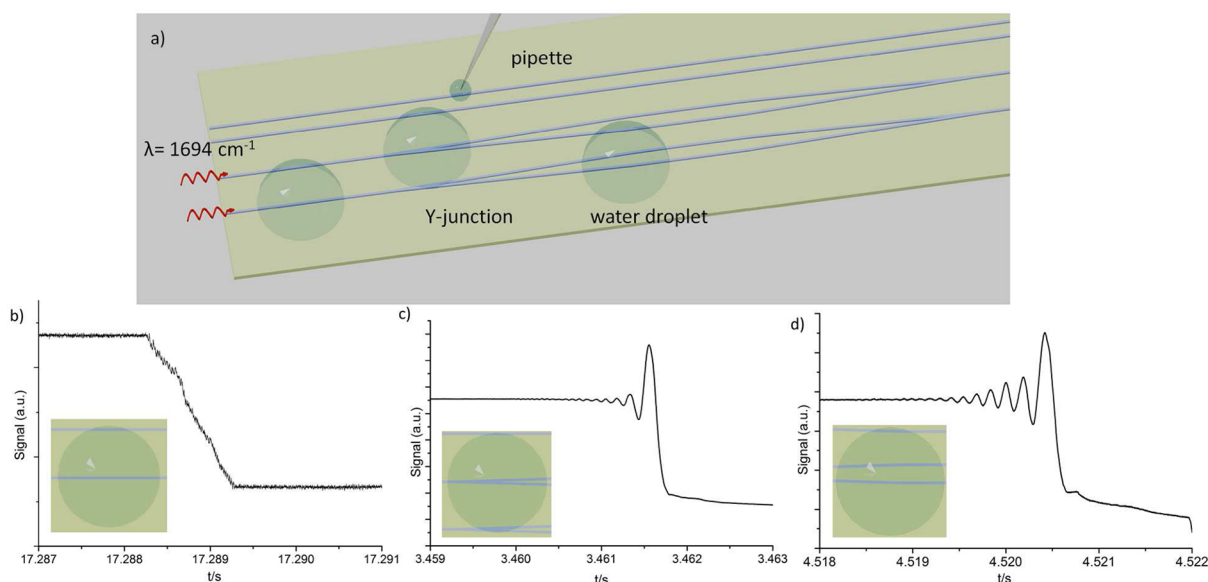


Figure 3. (a) Measurement scheme producing interferometric signals by depositing droplets of water (b) at the incoupling straight MZI waveguide, (c) at the Y-junction, and (d) at both arms of the MZI.

to the absorption of IR radiation by water at that wavelength was evident (Figure 3b). If droplets of water were deposited directly onto the arms of the MIR-MZI structure, a sizable interference signal was detected resulting from the change in refractive index during the deposition process (Figure 3d). If a water droplet was deposited directly onto the Y-junction (Figure 3c), only a shorter section of the MZI arms interact with the droplet, and the interference signal therefore decreases, as expected from the linear correlation between phase shift and interaction length. The droplets were present within the penetration depth of the evanescent field (extending approximately $6 \mu\text{m}$ along the MZI arm) within a few milliseconds, which is in agreement with the determined duration of the transient signals. The initial interference signal results from the change in humidity once the droplet is near the evanescent field, yet prior to deposition.

CONCLUSIONS

The first monolithically integrated on-chip Mach–Zehnder interferometers for the mid-infrared wavelength band based on GaAs/AlGaAs technology have been fabricated and tested. The developed MIR-MZI devices provide monomode optical behavior and exhibit exquisite surface sensitivity, which are necessary prerequisites for developing a new generation of chem-/biosensor platforms, taking advantage of the substantial penetration depth (i.e., several micrometers) of the evanescent field in the MIR and of the inherent molecular selectivity provided in this spectral window, in particular if combined with a tunable quantum cascade laser. It is anticipated that this optical diagnostic platform will allow one to study, e.g., protein conformation or (bio)molecular interactions in a label-free assay format yet using minute quantities of the probed molecules. Ongoing studies focus on the combination of MIR-MZI devices with microfluidic architectures and on the integration of grating structures for more efficient light coupling into the device.

AUTHOR INFORMATION

Corresponding Author

*E-mail: boris.mizaikoff@uni-ulm.de

Notes

The authors declare no competing financial interest.

ACKNOWLEDGMENTS

The authors gratefully acknowledge support of this study by the Kompetenznetz Funktionelle Nanostrukturen Baden Wuerttemberg, Germany.

REFERENCES

- Mizaikoff, B. *Anal. Chem.* **2003**, *75*, 258A–267A.
- Young, C.; Kim, S.-S.; Luzinova, Y.; Weida, M.; Arnone, D.; Takeuchi, E.; Day, T.; Mizaikoff, B. *Sens. Actuators, B* **2009**, *140*, 24–28.
- Chen, J.; Liu, Z.; Gmachl, C.; Sivco, D. *Opt. Express* **2005**, *13*, 5953–5960.
- Lechuga, L. M.; Sepulveda, B.; Sanchez del Rio, J.; Blanco, F.; Calle, A.; Dominguez, C. *Proc. SPIE* **2004**, *5357*, 96–110.
- Prieto, F.; Sepulveda, B.; Calle, A.; Llobera, A.; Dominguez, C.; Abad, A.; Montoya, A.; Lechuga, L. M. *Nanotechnology* **2003**, *14*, 907–912.
- Ingenhoff, J.; Drapp, B.; Gauglitz, G. *Fresenius' J. Anal. Chem.* **1993**, *346*, 580–583.
- Blanco, F. J.; Agirregabiria, M.; Berganzo, J.; Mayora, K.; Elizalde, J.; Calle, A.; Dominguez, C.; Lechuga, L. M. *J. Micromech. Microeng.* **2006**, *16*, 1006–1016.
- Charlton, C.; Giovannini, M.; Faist, J.; Mizaikoff, B. *Anal. Chem.* **2006**, *78*, 4224–4227.
- Wang, X.; Kim, S.-S.; Roßbach, R.; Jetter, M.; Michler, P.; Mizaikoff, B. *Analyst* **2012**, *137*, 2322–2327.
- Karlowatz, M.; Kraft, M.; Mizaikoff, B. *Anal. Chem.* **2004**, *76*, 2643–2648.